

Comparison of quantitative PCR and flow cytometry as cellular viability methods to study bacterial membrane permeabilization following supercritical CO₂ treatment

Sabrina Tamburini,¹ Annalisa Ballarini,¹ Giovanna Ferrentino,²
Albertomaria Moro,¹ Paola Foladori,³ Sara Spilimbergo²
and Olivier Jousson¹

Correspondence

Sabrina Tamburini
tamburini@science.unitn.it

¹Centre for Integrative Biology, University of Trento, 38123 Trento, Italy

²Department of Materials Engineering and Industrial Technologies, University of Trento, 38123 Trento, Italy

³Department of Civil and Environmental Engineering, University of Trento, 38123 Trento, Italy

Foodborne illness due to bacterial pathogens is increasing worldwide as a consequence of the higher consumption of fresh and minimally processed food products, which are more easily cross-contaminated. The efficiency of food pasteurization methods is usually measured by c.f.u. plate counts, a method discriminating viable from dead cells on the basis of the ability of cells to replicate and form colonies on standard growth media, thus ignoring viable but not cultivable cells. Supercritical CO₂ (SC-CO₂) has recently emerged as one of the most promising fresh food pasteurization techniques, as an alternative to traditional, heat-based methods. In the present work, using three SC-CO₂-treated foodborne bacteria (*Listeria monocytogenes*, *Salmonella enterica* and *Escherichia coli*) we tested and compared the performance of alternative viability test methods based on membrane permeability: propidium monoazide quantitative PCR (PMA-qPCR) and flow cytometry (FCM). Results were compared based on plate counts and fluorescent microscopy measurements, which showed that the former dramatically reduced the number of cultivable cells by more than 5 log units. Conversely, FCM provided a much more detailed picture of the process, as it directly quantifies the number of total cells and distinguishes among three categories, including intact, partially permeabilized and permeabilized cells. A comparison of both PMA-qPCR and FCM with plate count data indicated that only a fraction of intact cells maintained the ability to replicate *in vitro*. Following SC-CO₂ treatment, FCM analysis revealed a markedly higher level of bacterial membrane permeabilization of *L. monocytogenes* with respect to *E. coli* and *S. enterica*. Furthermore, an intermediate permeabilization state in which the cellular surface was altered and biovolume increased up to 1.5-fold was observed in *L. monocytogenes*, but not in *E. coli* or *S. enterica*. FCM thus compared favourably with other methods and should be considered as an accurate analytical tool for applications in which monitoring bacterial viability status is of importance, such as microbiological risk assessment in the food chain or in the environment.

Received 7 September 2012

Accepted 6 April 2013

INTRODUCTION

Foodborne illness is a public health challenge that, according to a World Health Organization report (WHO, 2007), caused almost 1.8 million human deaths in 2005

Abbreviations: FALS, forward angle light scatter; FCM, flow cytometry; FRET, fluorescence resonance energy transfer; gDNA, genomic DNA; LALS, large angle light scatter; PI, propidium iodide; PMA-qPCR, propidium monoazide quantitative PCR; SC-CO₂, supercritical CO₂; SYBR-I, SYBR Green I; VBNC, viable but not cultivable.

(Velusamy *et al.*, 2010). Such illness is mostly caused by eating food contaminated with pathogenic bacteria (e.g. *Escherichia coli* O157:H7, *Listeria monocytogenes*, *Salmonella enterica*), which enter the food supply through cross-contamination events or food handlers' poor hygiene. In particular, fresh or minimally processed fruit and vegetable products can easily become contaminated with pathogens along the food chain, from harvesting through transportation and processing, to handling. Food consumption patterns worldwide have now changed in favour of these

fresh (Anon, 2002) or minimally processed (Gandhi & Chikindas, 2007) ready-to-eat food products; as a consequence, the risk of foodborne illness is increasing.

Foodborne illnesses caused by fresh/minimally processed products can be prevented by applying pasteurization treatments aiming to reduce the number of viable pathogens without affecting food taste, appearance and quality. Thermal pasteurization procedures are highly effective, but they do not apply to fresh food products. Thus, non-thermal pasteurization methods have been developed, which inactivate microbes while not adversely compromising food integrity or nutritional quality, including high hydrostatic pressure and pulsed electrical fields (Devlieghere *et al.*, 2004), dense CO₂ or supercritical CO₂ (SC-CO₂) (Spilimbergo & Bertucco, 2003).

Among the latter methods, SC-CO₂ non-thermal pasteurization is one of the most promising for fresh food products. This method is based on the fluid state of CO₂ reached at or above its critical temperature and critical pressure. Compared with heat- and high hydrostatic pressure-based pasteurization, it has the advantage of working in a range of relatively low temperature (30–40 °C) and moderate pressure (80–120 bar), thus having a much lower impact on nutritional, organoleptic and physico-chemical properties of fresh/minimally processed food products (Garcia-Gonzalez *et al.*, 2007). The pasteurization efficiency of SC-CO₂ has been tested on several micro-organisms spiked into various substrates (Spilimbergo & Bertucco, 2003; Ferrentino & Spilimbergo, 2011). Specifically, treatments have led to a 3–4 log c.f.u. ml⁻¹ reduction in physiological saline buffer (Ballestra *et al.*, 1996; Erkmén, 2000; Erkmén & Karaman, 2001) and to a 2–2.5 log c.f.u. cm⁻² reduction on solid food products (Jung *et al.*, 2009; Bae *et al.*, 2011). The effect of SC-CO₂ on living cells has not been fully deciphered. Several hypotheses have been proposed based on experimental observations, including solubilization of pressurized CO₂ in the external liquid phase, cell membrane permeabilization, intracellular acidification, key enzyme inactivation/cellular metabolism inhibition due to pH lowering, direct (inhibitory) effect of molecular CO₂ and HCO₃⁻ on metabolism, disordering of the intracellular electrolyte balance, and removal of vital constituents from cells and cell membranes. Most of these steps may not occur consecutively, but rather take place simultaneously in a very complex and interrelated manner (Spilimbergo & Bertucco, 2003; Garcia-Gonzalez *et al.*, 2007).

To evaluate pasteurization efficiency, bacterial inactivation is typically deduced from c.f.u. plate counts, a viability test method measuring the bacterial ability to replicate and form colonies upon standard growth conditions. It is well known that, under environmental stress conditions (e.g. nutrient limitation, pressure, temperature), a number of pathogens enter into a so-called viable but not cultivable state (VBNC), becoming even more resistant to stress (Oliver, 2010). Thus, plate counts may overestimate pasteurization efficiency, by not

detecting as viable reversibly damaged bacterial cells (Keer & Birch, 2003).

Additional viability test methods may be more suited for studying the efficiency of pasteurization treatment on bacterial cells, including propidium monoazide quantitative PCR (PMA-qPCR) (Nocker & Camper, 2006) and flow cytometry (FCM) (Müller & Nebe-von-Caron, 2010). Both methods employ cell-membrane permeability as the viability parameter. PMA-qPCR is a quantitative PCR amplification performed after PMA staining, an analogue of propidium iodide (PI) with a covalently linked azide group, used as a marker of bacterial cells with a permeabilized membrane. After photoactivation, PMA binds irreversibly to dsDNA, thus inhibiting DNA amplification during qPCR or causing DNA loss with cellular debris during DNA extraction. PMA was used to discriminate intact and permeabilized cells in an environmental matrix (Nocker *et al.*, 2007a) and was applied to monitor the effect of disinfection treatments altering membrane integrity (Nocker *et al.*, 2007b).

FCM is a multi-parametric and single-cell analysis technique for high-throughput and real-time quantification of multiple cellular parameters, such as cell size, surface granularity and physiological state. In FCM, two light-scattering signals can be collected simultaneously from each bacterial cell: the forward-angle light scatter (FALS), which is related to bacterial size (Foladori *et al.*, 2008), and the large-angle light scatter (LALS), measuring cell density or granularity (Müller & Nebe-von-Caron, 2010). In FCM studies, the fluorophore SYBR Green I (SYBR-I) is often used as a total cell marker, given its ability to cross the cell membrane and to bind to DNA (Barbesti *et al.*, 2000), whilst PI is used as a dead cell marker, as it penetrates only cells with a permeabilized membrane (Ziglio *et al.*, 2002). In permeabilized cells the simultaneous presence of SYBR-I and PI activates fluorescence resonance energy transfer (FRET), due to the total absorption of the fluorescent emission spectrum of SYBR-I by PI. In these conditions, it is therefore possible to distinguish intact cells emitting green fluorescence from permeabilized ones emitting red fluorescence. FCM coupled with fluorescent dyes (SYBR-I and PI or Syto9 and PI) was used to discriminate intact and permeabilized cells in a wastewater treatment plant (Foladori *et al.*, 2010) and to monitor the effect of various antibacterial treatments (Wouters *et al.*, 2001; Kim *et al.*, 2009).

In the present work, *L. monocytogenes*, *E. coli* and *S. enterica* were treated with SC-CO₂ to evaluate the performance of different cell viability assays. Data from FCM and PMA-qPCR were compared with plate counts and fluorescent microscopy, to evaluate which method is the most appropriate to correctly discriminate viable from dead cells after treatment.

METHODS

Bacterial strains and sample preparation. The three strains used in this study were purchased from the American Type Culture

Collection. *S. enterica* ATCC 14028 and *E. coli* ATCC 29522 were grown on solid Luria–Bertani (LB) agar medium (Sigma-Aldrich) at 37 °C for 16 h. *L. monocytogenes* ATCC 19111 was grown on solid brain heart infusion (BHI) medium (Becton Dickson) at 37 °C for 16 h. One colony was picked and inoculated into 200 ml of corresponding broth medium. Bacterial cultures were incubated at 37 °C with constant shaking (200 r.p.m.) to stationary phase (16 h). Cells were collected by centrifuging at 6000 r.p.m. for 10 min and were resuspended in an equal volume of PBS (Sigma-Aldrich).

SC-CO₂ treatment. The SC-CO₂ treatment was performed in a multi-batch apparatus as described by Mantoan & Spilimbergo (2011). Briefly, the system consisted of 10 identical 15 ml-capacity reactors operating in parallel. All reactors were submerged in the same temperature-controlled water bath to maintain the desired temperature constant throughout the process. Each reactor was connected to an on-off valve for independent depressurization and had an internal magnetic stirrer device to guarantee homogeneous dissolution in the cell suspension. Aliquots of 10 ml of each bacterial suspension, prepared as described above, were transferred to the reactors. The SC-CO₂ treatment was carried out at 120 bar and 35 °C, as these operative conditions were selected in preliminary plate counts experiments as the mildest ones that induced significant microbial inactivation. SC-CO₂ treatment was interrupted after 5, 15, 30, 45 or 60 min by slowly depressurizing the reactor over approximately 1 min.

Plate counts. Untreated and SC-CO₂-treated cells were serially diluted with 1 × PBS (900 µl PBS and 100 µl sample) and were spread-plated on chromogenic coli/coliform agar (Liofilchem) for *E. coli*, on chromatic Salmonella agar (Liofilchem) for *S. enterica* and on O.A. Listeria agar (Liofilchem) for *L. monocytogenes*. The plates were incubated at 37 °C for 24 h. Three independent experiments were performed for each species.

Fluorescence microscopy. In total, 10⁸ untreated or SC-CO₂-treated cells were stained with SYBR-I and PI, as described for FCM. After staining, cells were centrifuged at 10 000 r.p.m. for 10 min and the pelleted cells were resuspended in 1 × PBS and 30 % Moviol. Fluorescence microscopy images were acquired in bright-field at 490 and 750 nm, with a ZeissAxio Observer Z.1 microscope with Zeiss ApoTome device using the AxioVision Rel. 4.8.1 software (Zeiss) according to the manufacturer's instructions.

Genomic DNA extraction and PMA staining. In total, 10⁷–10⁸ untreated or treated cells were stained with PMA (Biotium), at a final concentration of 50 µM, and incubated at room temperature in the dark for 5 min. Stained samples were then exposed to UV light for 5 min and centrifuged for 10 min at 12 000 r.p.m. Cell pellets were stored at –20 °C. Genomic DNA (gDNA) was extracted from unstained and PMA-stained samples using a Qiagen DNeasy Blood and Tissue kit, according to the manufacturer's instructions. A modified protocol was used for *L. monocytogenes*: cells were incubated at 37 °C for 1 h with the enzymic lysis buffer provided by the supplier. Cells were then incubated at 56 °C for 30 min and were treated with RNase A. After column purification, DNA was eluted with 100 µl 10 mM Tris/HCl, pH 8.0. DNA quality was assessed by 0.7 % agarose gel electrophoresis, run at 70 V for 30 min and followed by ethidium bromide staining. DNA concentration and purity were assessed by measuring the absorbance at 260 nm (A_{260}) and the ratio of the absorbance at 260 and 280 nm (A_{260}/A_{280}) with a NanoDrop ND-1000 spectrophotometer (Thermo Scientific).

Real-time qPCR. Primer and TaqMan probe set sequences targeting the *hlyA* and the *invA* genes were used for *L. monocytogenes* and *S. enterica* identification, respectively (Suo *et al.*, 2010). The best candidate primers and probe sets for *E. coli* identification were designed in-house on the *uidA* marker gene with AlleleID7.0 software

(PREMIER Biosoft International). Primer sequences and their features are detailed in Table 1. The reaction mixture contained 1 × iQ Multiplex Powermix (Bio-Rad Laboratories), 200 nM each primer, 200 nM probe and 2 µl template gDNA (or 2 µl distilled H₂O for the no-template control) in a total volume of 25 µl. Each TaqMan PCR assay was performed in triplicate using a CFX96 Real-time PCR Detection System (Bio-Rad Laboratories), with the following cycling programme: 3 min at 95 °C, 15 s at 95 °C and 1 min at 60 °C for 40 cycles. PCR results were analysed using CFX Manager 1.1 software (Bio-Rad Laboratories). The correlation between PCR *Ct* values and gene copy numbers was obtained by means of a standard curve. Cell number equivalents were then extrapolated by taking into account the mean bacterial genome size for each target bacterium available at NCBI (http://www.ncbi.nlm.nih.gov/genomes/MICROBES/microbial_taxtree.html), assuming each gene is present in a single copy per genome. The number of gDNA copies for experimental samples was determined by using the inverse formula of linear equation of each species ($\text{DNA copies} = 10^{(Ct - q) \cdot m - 1}$). The amplification efficiency for each primer/probe set was calculated as $E = 10^{(-1/\text{slope})} - 1$ (Klein, 2002). Assays were performed in parallel on cell suspensions before and after PMA staining to quantify total and intact cell number equivalents, respectively.

Flow cytometry. Untreated and SC-CO₂-treated cell suspensions were diluted to 10⁷–10⁸ cells ml⁻¹; then 1 ml was stained with 10 µl SYBR-I (Merck), 1 : 30 000 final concentration in DMSO, and 10 µl PI 1 mg ml⁻¹ (Invitrogen). Peak excitation and emission wavelengths were at $\lambda_{\text{ex}} = 495$ nm, $\lambda_{\text{em}} = 525$ nm for SYBR-I and $\lambda_{\text{ex}} = 536$ nm, $\lambda_{\text{em}} = 617$ nm for PI. Samples were incubated at room temperature in the dark for 15 min. FCM analyses were performed with an Apogee-A40 flow cytometer (Apogee Flow Systems) equipped with an argon laser emitting at 488 nm. For each cell crossing the focus point of the laser, two light-scattering signals (FALS and LALS) and two fluorescence signals (red and green) were collected. LALS and FALS were collected on a 256-channel linear scale while fluorescence signals were collected with logarithmic amplifier gain. The conversion of FALS intensities to biovolumes was performed as proposed by Foladori *et al.* (2008). To exclude electronic noise, thresholds were set on green or red fluorescence histograms.

RESULTS

Cell viability evaluated by plate counts and fluorescence microscopy

The efficiency of SC-CO₂ treatment was evaluated by quantifying bacterial cells able to replicate using plate counts and observing PI uptake by fluorescence microscopy (Fig. 1). To compare the efficiency of treatment among the tested species, the bacterial inactivation was expressed as $\log_{10}(N_t/N_0)$, as a function of treatment time (Fig. 1a). After 5 min, only *S. enterica* cells showed more than 1 log reduction. After 30 min the process dramatically reduced the number of cultivable cells by more than 5 log in all three species. An increase of treatment time up to 60 min did not induce any additional significant inactivation.

Bacterial inactivation on the basis of PI uptake as a function of treatment time was evaluated by using fluorescent staining of SYBR-I and PI. Fluorescence microscopy images of untreated and treated bacterial cells (Fig. 1b) showed a significant shift from green fluorescence to yellow/red fluorescence after 30 min treatment: almost

Table 1. Gene targets, primers and probes used for qPCR

Dyes refer to the reporter and quenching fluorophores linked to the TaqMan probe sequences.

Oligo name	Gene target	Sequence (5'–3')	T_m (°C)*	Dye (5'–3')	Reference
EC-uidAF	<i>uidA</i>	CTCTGCCGTTTCCAAATC			This work
EC-uidAR		GAAGCAACGCGTAAACTC			
EC-uidAP		AATGTAATGTTCTGCGACGCTCAC			
SE-invAF	<i>invA</i>	GTTGAGGATGTTATTTCGCAAAGG	70.1	HEX/BHQ1	Suo <i>et al.</i> (2010)
SE-invAR		GGAGGCTTCCGGGTCAAG			
SE-invAP		CCGTCAGACCTCTGGCAGTACCTTCCTC			
LM-hlyAF	<i>hlyA</i>	ACTGAAGCAAAGGATGCATCTG			Suo <i>et al.</i> (2010)
LM-hlyAR		TTTTCGATTGGCGTCTTAGGA			
LM-hlyAP		CACCACCAGCATCTCCGCCTGC			

* T_m , Melting temperature.

all *L. monocytogenes* cells emitted yellow/red fluorescence whilst *E. coli* and *S. enterica* cells emitted green, yellow and red fluorescence.

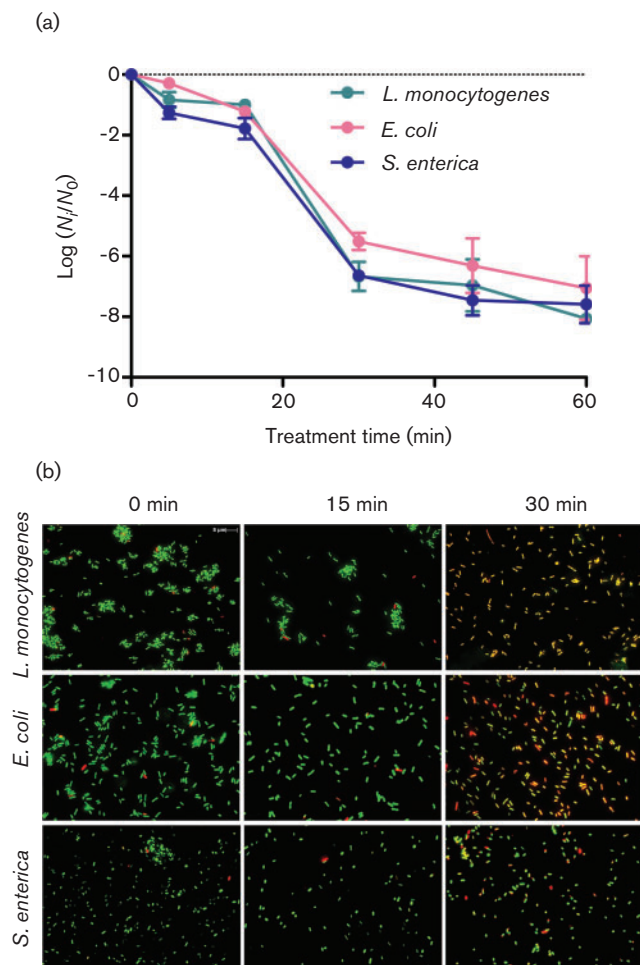


Fig. 1. Bacterial inactivation following SC-CO₂ treatment evaluated by (a) plate counts expressed as logN_t/N₀ and (b) fluorescence microscopy after staining by SYBR-I and PI.

Bacterial membrane permeabilization evaluated by PMA-qPCR

TaqMan qPCR analyses were performed on gDNA samples extracted from cell suspensions before and after PMA staining, to quantify both total and intact cell unit equivalents. qPCR data for each bacterial species revealed that the fraction of intact cells from all three species was reduced to less than 50% cell equivalents. However, such reduction was reached after different treatment time periods: 30–45 min for *L. monocytogenes*, 15–30 min for *E. coli* and 5–15 min for *S. enterica* (Table 2). After 5 min, *L. monocytogenes* intact cells showed a 10% reduction, whereas *E. coli* and *S. enterica* intact cells showed a 20 and 35% reduction, respectively. After the longest treatment time (60 min), the proportion of permeabilized cells was 82.4% for *L. monocytogenes*, 66.6% for *E. coli* and 41.9% for *S. enterica*.

Detection of intact and permeabilized cells by FCM

Upon staining of a mixed population of intact and permeabilized cells with SYBR-I and PI, FCM distinguishes among three cellular states: (i) intact cells, emitting only high FL1 intensity due to the absence of intracellular PI; (ii) partially permeabilized cells emitting high fluorescent intensity both in FL1 and in FL3 channels, due to incomplete FRET between SYBR-I and intracellular PI; and (iii) permeabilized cells emitting only high FL3 intensity, due to the simultaneous presence of SYBR-I and PI in the cells and complete FRET. Analyses were performed on cell suspensions stained with both SYBR-I and PI for quantification of total and permeabilized cells, respectively. The observed kinetics of cell membrane permeabilization was specific for each bacterial species (Table 3). With regard to *L. monocytogenes*, the percentage of intact cells was 99.5% in the untreated suspension, but this decreased significantly with treatment time. After 5 min, a small fraction of cells (1.3%) were partially permeabilized. After 30 min, the number of partially permeabilized cells reached its maximum, i.e. 17.2% of total cells, whereas the percentage of

Table 2. Target gene copy numbers determined by qPCR following SC-CO₂ treatment

Mean (\pm SD) target-gene copy number were determined in triplicate for each species and each treatment time. The percentages of intact cells reduction were calculated as the ratio of treated PMA-stained cells relative to untreated. NA, Not applicable.

Species and fluorophores	Treatment time (min)	Target gene copy numbers		
		-PMA (total cell equivalents)	+PMA (intact cell equivalents)	% Intact cells reduction
<i>L. monocytogenes</i> <i>hlyA</i> (Texas Red)	0	$5.24 \times 10^7 \pm 0.86$	$7.28 \times 10^7 \pm 0.30$	NA
	5	$4.91 \times 10^7 \pm 0.67$	$6.81 \times 10^7 \pm 0.62$	6.43 ± 6.41
	15	$4.89 \times 10^7 \pm 0.45$	$4.88 \times 10^7 \pm 0.10$	32.92 ± 4.80
	30	$4.92 \times 10^7 \pm 0.89$	$4.91 \times 10^7 \pm 0.71$	32.55 ± 7.60
	45	$9.46 \times 10^7 \pm 2.06$	$0.69 \times 10^7 \pm 0.57$	90.39 ± 5.63
	60	$9.37 \times 10^7 \pm 1.02$	$1.27 \times 10^7 \pm 0.23$	82.44 ± 6.06
<i>E. coli</i> <i>uidA</i> (HEX)	0	$1.89 \times 10^8 \pm 0.73$	$2.21 \times 10^8 \pm 0.19$	NA
	5	$1.45 \times 10^8 \pm 0.37$	$1.73 \times 10^8 \pm 0.25$	22.04 ± 10.85
	15	$1.33 \times 10^8 \pm 0.52$	$1.78 \times 10^8 \pm 0.16$	19.57 ± 12.00
	30	$0.80 \times 10^8 \pm 0.48$	$0.47 \times 10^8 \pm 0.17$	78.54 ± 10.90
	45	$0.87 \times 10^8 \pm 0.09$	$0.80 \times 10^8 \pm 0.06$	63.55 ± 13.10
	60	$0.90 \times 10^8 \pm 0.25$	$0.74 \times 10^8 \pm 0.20$	66.55 ± 11.20
<i>S. enterica</i> <i>invA</i> (FAM)	0	$3.78 \times 10^8 \pm 0.18$	$5.62 \times 10^8 \pm 4.12$	NA
	5	$3.44 \times 10^8 \pm 1.20$	$3.47 \times 10^8 \pm 0.49$	34.57 ± 10.51
	15	$2.57 \times 10^8 \pm 0.13$	$2.51 \times 10^8 \pm 0.00$	55.36 ± 13.24
	30	$3.00 \times 10^8 \pm 0.12$	$3.11 \times 10^8 \pm 0.39$	44.66 ± 11.45
	45	$3.77 \times 10^8 \pm 0.13$	$3.73 \times 10^8 \pm 0.58$	33.66 ± 13.02
	60	$3.65 \times 10^8 \pm 1.10$	$3.27 \times 10^8 \pm 0.43$	41.85 ± 14.07

intact cells decreased but remained high (71.2%). After 45 min, the percentages of both intact and partially permeabilized cells decreased significantly and almost all cells (96.4%) were fully permeabilized.

The untreated *E. coli* and *S. enterica* bacterial suspensions contained 99.8 and 98.6% of intact cells, respectively. As for *L. monocytogenes*, after 5 min of treatment a small percentage of cells (3.0 and 4.8%, respectively) became partially permeabilized, while a negligible amount of dead cells was detected. After 15 min, *E. coli* subpopulations maintained the same distribution, with 96.2% of intact cells and 3.6% of partially permeabilized cells. By contrast, almost all *S. enterica* cells were split between intact (59.9%) and partially permeabilized (39.6%). After 30 min, a similar behaviour was observed for *E. coli* and *S. enterica* populations: a large percentage of cells were partially permeabilized (95.3 and 93.7%, respectively) but almost no totally permeabilized cells were detected. Longer SC-CO₂ treatment times did not lead to significant changes in population distribution, as the vast majority of cells (99.2%) from both species remained in the partially permeabilized state.

Investigation of subpopulations of partially permeabilized cells by FCM

The kinetics of cell inactivation was further investigated by FCM, examining the variation over time in SYBR-I and PI

uptake in SC-CO₂-treated samples. As shown in Fig. 2, *L. monocytogenes*, *E. coli* and *S. enterica* differed in their SYBR-I uptake kinetics, as shown by the green fluorescence intensity (FL1 channel) at each treatment time point. For example, the intensity measured in the FL1 median channel for *L. monocytogenes* was constant for treatment-time extensions from 5 to 30 min (Fig. 2a). The graph of FL1 intensity showed limited variations in the FL1 median channel, which ranged from 402 to 412 units based on the arbitrary 1024-channel scale. This result indicates that the uptake of SYBR-I in *L. monocytogenes* is complete even in the untreated cells. For treatment times higher than 45 min, the FL1 median channel decreased to 202–220 units, due to the large percentage of permeabilized cells, in which FRET (i.e. quenching of FL1 fluorescence by PI) occurred.

Conversely, the FL1 intensity of intact cells in untreated samples of *E. coli* was weak and close to the threshold of FL1-positive signals (Fig. 2b) due to partial staining of cells by SYBR-I. By increasing SC-CO₂ treatment time, both *E. coli* and *S. enterica* populations showed a progressive and significant increase of FL1 intensity, corresponding to a shift of the FL1 histogram peak from left to right and to an increase in peak intensity far above the background threshold of the instrument (Fig. 2b,c). *E. coli* and *S. enterica* populations reached their maximum value of FL1 median channel after 45 and 15 min, respectively. This

Table 3. Membrane permeabilization determined by FCM following SC-CO₂ treatment

Bacterial species	Treatment time (min)	Intact cells* (%)	Partially permeabilized cells† (%)	Permeabilized cells‡ (%)
<i>L. monocytogenes</i>	0	99.5	0.2	0.2
	5	97.4	1.3	1.3
	15	96.2	1.7	2.0
	30	71.2	17.2	11.0
	45	0.5	3.1	96.4
	60	0.5	7.3	92.2
<i>E. coli</i>	0	99.8	0.2	0.1
	5	96.8	3.0	0.2
	15	96.2	3.6	0.2
	30	4.5	95.3	0.2
	45	7.5	92.1	0.2
	60	0.3	99.2	0.2
<i>S. enterica</i>	0	98.6	1.0	0.3
	5	94.9	4.8	0.2
	15	59.9	39.6	0.3
	30	5.9	93.7	0.3
	45	11.5	88.0	0.3
	60	0.3	99.2	0.5

*Intact cells emitting only high FL1 intensity.

†Partially permeabilized cells emitting high fluorescent intensity in both FL1 and FL3 channels.

‡Permeabilized cells emitting only high FL3 intensity.

progressive increase in FL1 emission in *E. coli* and *S. enterica* is probably due to the gradual permeabilization of cells during SC-CO₂ treatment, which facilitated the uptake of SYBR-I.

As shown in Fig. 3, for the *E. coli* population, the presence of a subpopulation with high FL1 intensity was negligible in untreated samples, whereas it was detectable (15.2%) after 5 min of treatment and dominant (86%) after 30 min. Among the 15.2% of *E. coli* cells with higher FL1 intensity after 5 min, 12.0% represented intact cells whilst 3.2% were partially permeabilized cells. After 30 min, the progressive staining by PI resulted in 95.3% of partially permeabilized cells, with a fraction of 86% with high FL1 intensity.

With regard to the *S. enterica* population, the FL1 intensity increased significantly in a group of cells after 15 min of treatment. This subpopulation moved to the right on the FL1 graph, being characterized by a higher SYBR-I uptake (Fig. 4). Only cells with initial high FL1 intensity moved towards the region of partially permeabilized cells. These results suggest that the treatment led first to the progressive introduction of SYBR-I with the complete staining of cells and the emission of high FL1 intensity, and, later, when the membrane became more permeable, to the progressive and partial staining of cells by PI. The co-occurrence of green and red fluorescence is probably a consequence of incomplete FRET occurring between SYBR-I and PI, due to a lower PI uptake.

Interestingly, while the group of cells with low SYBR-I concentration exhibited a unimodal distribution, the group of cells with high SYBR-I concentration was characterized

by a noticeable bimodal distribution (Fig. 4) corresponding to two subpopulations with different amounts of DNA. The ratio of the FL1 intensity (high DNA peak/low DNA peak ratio) was about 1.5. Additionally, the FALS ratio of the two subpopulations was 1.4, indicating a larger brighter fluorescent peak, therefore confirming that the subpopulation of bacteria with a larger amount of DNA also had a larger biovolume. FL1 intensity and FALS ratios indicated that these cells are dividing actively.

Morphological changes evaluated by LALS and FALS FCM signals

The light-scattering signals collected by the flow cytometer, i.e. FALS and LALS, are related to physical properties of the bacteria. In particular, FALS depends on bacterial size (and cellular biovolume) while LALS is related to the complexity of the cellular surface, cell density and granularity. The FALS and LALS signals of *E. coli* and *S. enterica* populations did not change significantly over treatment time (data not shown). Conversely, *L. monocytogenes* cells showed changes in both light-scattering signals at different treatment times. In particular, although the scattering signals of intact and permeabilized *Listeria* cells were similar, as demonstrated by the overlapping distributions in Fig. 5, the partially permeabilized cells were characterized by a higher FALS intensity (larger size) and slightly higher LALS intensity. With reference to an arbitrary scale of 1024 channels, the peaks of the FALS distribution of intact and permeabilized cells of *L. monocytogenes* were at channels 187 and 133, respectively, whereas the peak of partially permeabilized cells

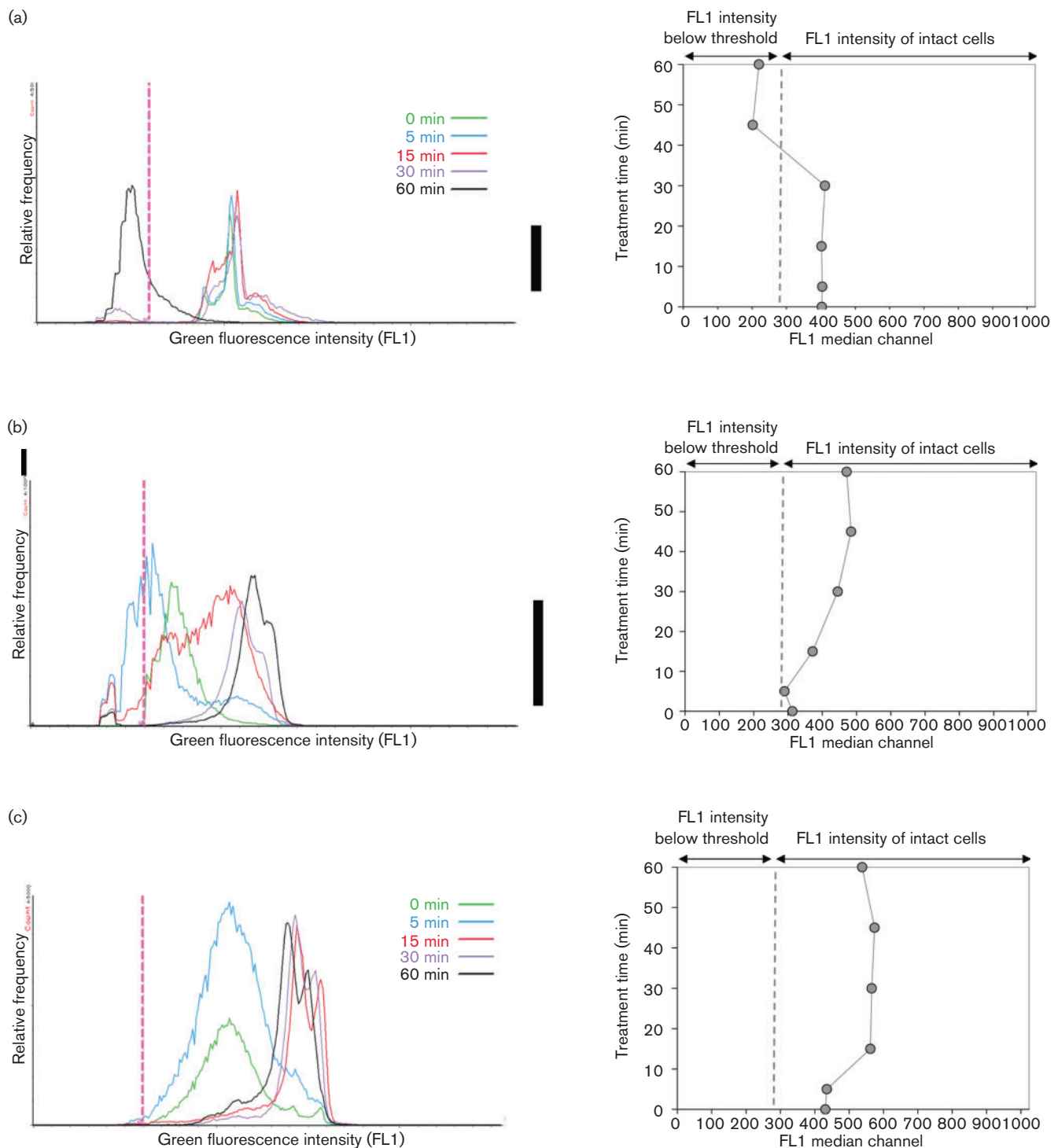


Fig. 2. FCM analysis showing SYBR-I uptake by *L. monocytogenes* (a), *E. coli* (b) and *S. enterica* (c) cells over treatment time. FL1 signal distribution for each treatment time (left) and corresponding FL1 median channels values (right) are shown.

was at channel 398. Conversion of FALS intensities produced a biovolume ratio of about 1.5 between partially permeabilized and intact cells. This ratio, together with the increase in LALS intensity, indicates that bacteria temporarily underwent a pronounced increase in biovolume.

Correlation between plate counts, qPCR and FCM methods in evaluating cell viability

We compared the concentration of viable cells obtained by plate counts with that of intact cells determined by PMA-qPCR and FCM during SC-CO₂ treatment. The three

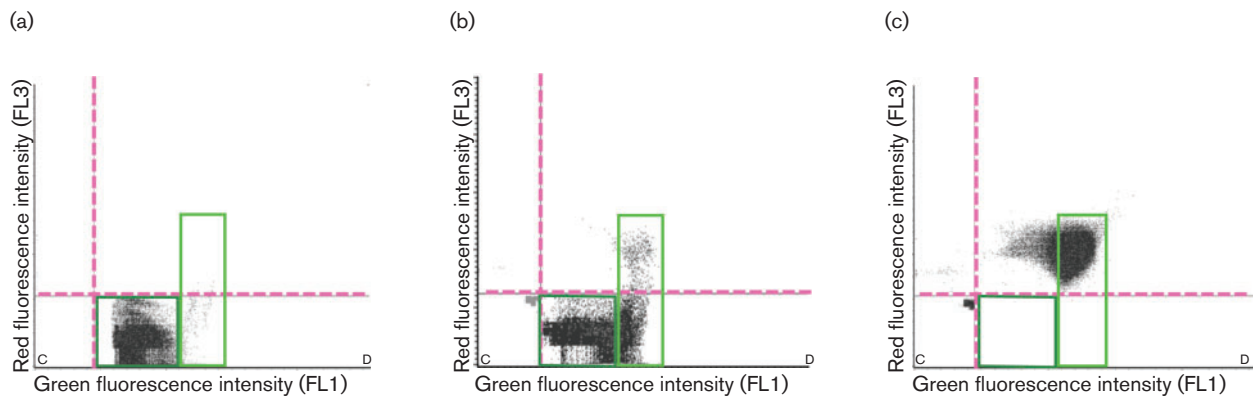


Fig. 3. High- and low-fluorescence subpopulations detected by FCM within *E. coli* populations after SC-CO₂ treatment. FL1–FL3 dot plots were obtained by measuring red versus green fluorescence in (a) untreated, (b) 5 min-treated and (c) 30 min-treated *E. coli* cell suspensions. Cell subpopulations characterized by low and high SYBR-I uptake are bordered by dark and light green boxes, respectively.

methods produced similar results during the initial phase (15 min) (Fig. 6). After 30 min, a dramatic decrease (>5 log) in the number of viable cells was observed with plate counts, whereas FCM and, in particular, qPCR showed a much more modest reduction of intact cells (about 0.9 and 0.5 log, respectively), indicating that only a small fraction of intact cells (as determined by FCM and qPCR) are effectively able to replicate *in vitro* (as determined by plate counts) after treatment.

To determine if the three methods produced consistent and comparable results, Pearson correlation coefficients (r) were calculated (Fig. 7). The highest correlation was between qPCR and FCM for *L. monocytogenes* and *E. coli*

($r=0.91$ and 0.92 , respectively), and between qPCR and plate counts for *S. enterica* ($r=0.92$). The poorest correlations were between FCM and plate counts for both *E. coli* and *S. enterica* ($r=0.60$ and 0.62 , respectively), and between qPCR and plate counts for *L. monocytogenes* ($r=0.63$).

DISCUSSION

In this study we compared different viability assays to monitor the efficiency of SC-CO₂ treatment on *L. monocytogenes*, *E. coli* and *S. enterica*. Plate counts showed that the treatment inactivated viable cells by >5 log.

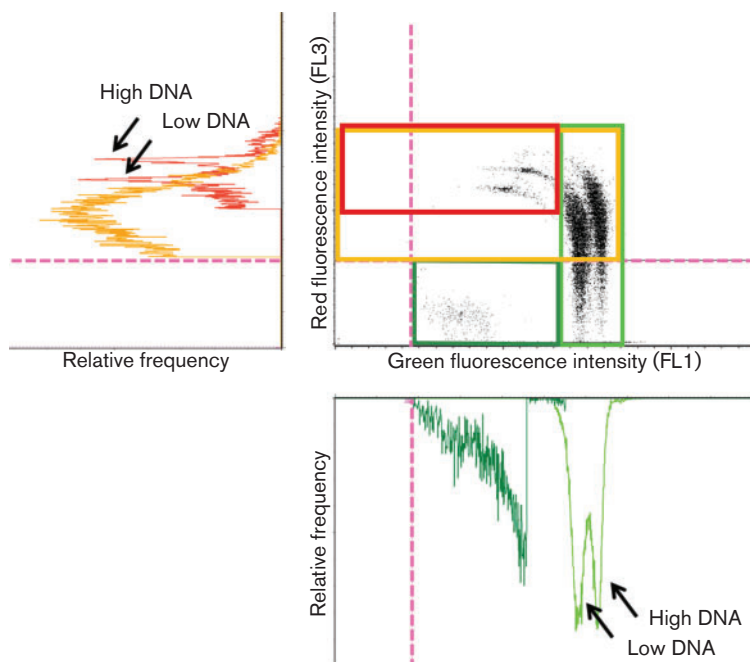


Fig. 4. Cell subpopulations identified by FCM in *S. enterica* cell suspensions after 15 min of SC-CO₂ treatment. Cells with low and high SYBR-I uptake are bordered by light and dark green boxes, respectively, whereas cells with low and high PI uptake are bordered by yellow and red boxes, respectively. The single channel distributions are shown next to their corresponding fluorescence channel. Arrows indicate cell subpopulations with low and high DNA content.

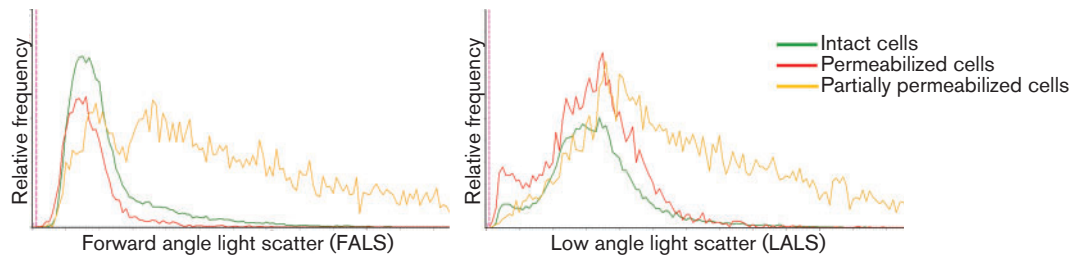


Fig. 5. FALS (left) and LALS (right) signal distributions evaluated by FCM analysis on *L. monocytogenes* cells treated for 30 min with SC-CO₂.

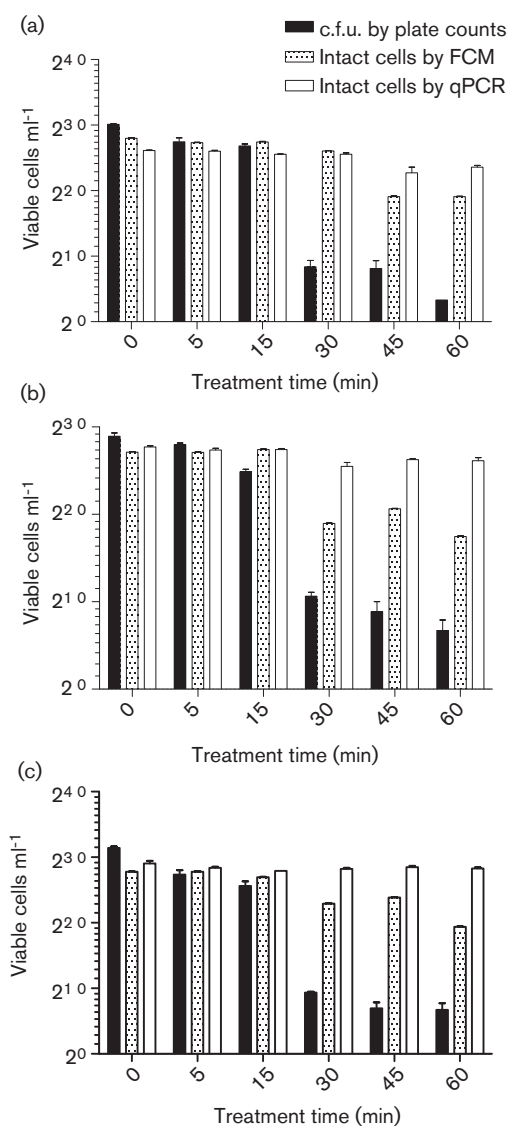


Fig. 6. Number of viable or intact cells monitored during SC-CO₂ treatment and inferred from plate counts, qPCR and FCM for *L. monocytogenes* (a), *E. coli* (b) and *S. enterica* (c). Error bars represent standard deviations from three independent replicates.

Fluorescence microscopy globally corroborated plate count data, with a marked bacterial permeabilization process revealed by PI uptake after 30 min treatment. Under environmental stress, many bacteria are known to enter in a so-called VBNC state, becoming even more resistant to stress (Oliver, 2010). Plate counts therefore probably overestimate bacterial inactivation, as VBNC cells escape detection by cultural methods. We applied two viability methods based on membrane integrity (PMA-qPCR and FCM) to overcome the limits of plate counts and to identify the proportion of VBNC cells in the populations. We showed that qPCR and FCM produced strongly correlated results for two out of three bacterial species tested, which was expected as both methods quantify cellular subpopulations on the basis of membrane permeability. Our results also confirmed that plate counts drastically underestimate the number of intact cells, being unable to detect those in a VBNC state.

According to Nocker *et al.* (2007b), PMA-qPCR is an adequate tool to monitor the effect of a given treatment affecting bacterial membrane integrity. PMA-qPCR produced inconsistent data to evaluate the efficiency of the treatment on *S. enterica*, while it correctly detected the effect of SC-CO₂ on *L. monocytogenes* and *E. coli*, supporting previously published data (Garcia-Gonzalez *et al.*, 2010). qPCR is a highly sensitive method able to detect fewer than 10 genome equivalents per reaction and is therefore the technique of choice for quantification of micro-organisms at low concentrations. A main disadvantage of PMA-qPCR applied to bacterial viability studies lies in the fact that variations in genomic DNA extraction and PMA-staining efficiency may cause biases in the determination of the number of intact cells.

Conversely, FCM coupled with SYBR-I and PI staining provided consistent and detailed information on the cell permeabilization process. This technique distinguished cells in three different states: intact, partially permeabilized and permeabilized. FCM analyses highlighted a diverse effect of the treatment on *L. monocytogenes* compared with *E. coli* and *S. enterica*. After 30 min treatment, 71.2% of *L. monocytogenes* cells were intact, whereas 95.3% of *E. coli* and 93.7% of *S. enterica* cells were partially permeabilized.

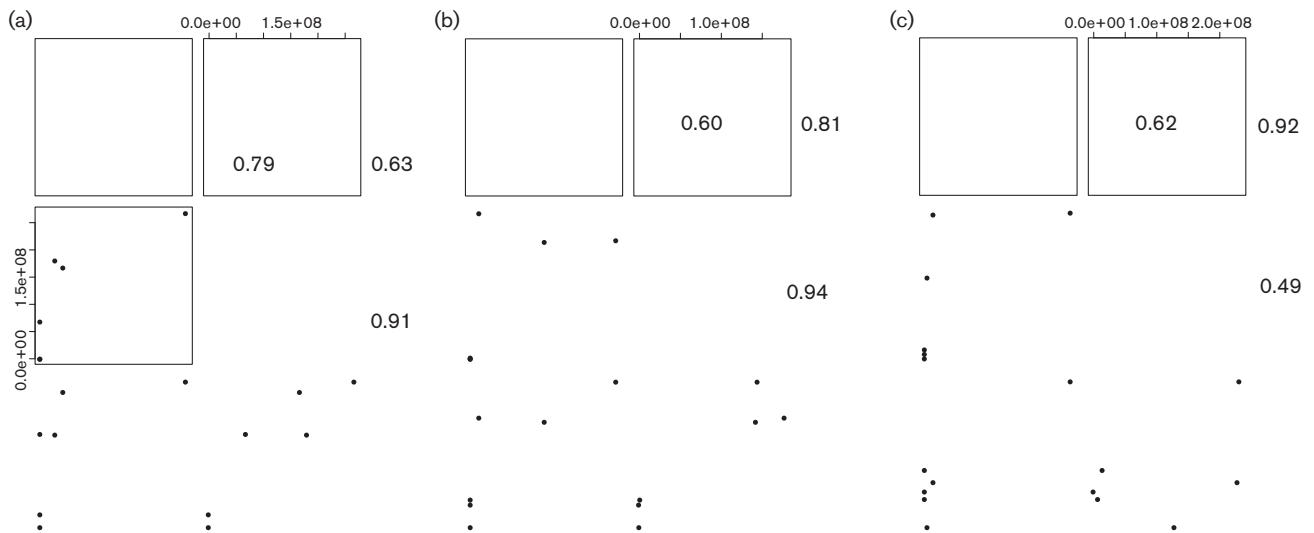


Fig. 7. Pairwise correlation analysis of plate counts, PMA-qPCR and FCM in estimating the number of viable or intact cells after SC-CO₂ treatment for *L. monocytogenes* (a), *E. coli* (b) and *S. enterica* (c).

By contrast, the fraction of cultivable cells was reduced by more than 5 log for all three species.

FCM estimated the variation of FL1 intensity during treatment in *E. coli* and *S. enterica*, indicating a gradual permeabilization of cells and facilitating the uptake of SYBR-I, as suggested by Liao *et al.* (2010). The emergence of subpopulations of cells with double the amount of DNA appeared only when SYBR-I completely entered the cells, in agreement with data reported by Berney *et al.* (2007) with SYTO-9. The double amount of DNA was detected both in partially permeabilized cells and in almost totally permeabilized cells, as shown by the overlapping green and red fluorescence peaks in the FL1 and FL3 channels, respectively. The ability of the fluorescent dyes to enter the cells depends on the level of outer membrane permeabilization for SYBR-I and on the level of both outer and cytoplasmic membrane permeabilization for PI. The double amount of DNA was not observed in the intact and permeabilized cells from the untreated sample, presumably due to limitations in the diffusion of SYBR-I across the membranes. In addition, a shift of both FALS and LALS signals in partially permeabilized *L. monocytogenes* cells suggested a temporary increase of biovolume and surface alteration during permeabilization, while in *E. coli* and *S. enterica* the process did not affect biovolume or cellular surface.

The FCM assay showed the best performance as a bacterial viability test method, evaluated here by monitoring membrane permeabilization following SC-CO₂ treatment. FCM allowed us not only to quantify the efficiency of treatment rapidly and with high sensitivity, but also to discriminate the subpopulations of partially permeabilized cells from totally permeabilized cells and identify variations in biovolume and alterations of the cellular surface. FCM compared favourably with other methods and should be

considered as an accurate analytical tool for applications in which monitoring bacterial viability status is of importance, such as microbiological risk assessment in the food chain or in the environment.

ACKNOWLEDGEMENTS

S. T. and G. F. were supported by the European Community's Seventh Framework Program (FP7/2007–2013) under grant agreement no. 245280, acronym PRESERF: 'Processing Raw Materials into Excellent and Sustainable End products while Remaining Fresh'. We thank Nicola Segata for providing support with statistical analyses.

REFERENCES

- Anon (2002). *Risk profile on the microbiological contamination of fruits and vegetables eaten raw: Report of the Scientific Committee on Food*. Brussels: SCF/CS/FMH/SURF.
- Bae, Y. Y., Choi, Y. M., Kim, M. J., Kim, K. H., Kim, B. C. & Rhee, M. S. (2011). Application of supercritical carbon dioxide for microorganism reduction in fresh pork. *J Food Saf* **31**, 511–517.
- Ballestra, P., Abreu da Silva, A. & Cuq, J. L. (1996). Inactivation of *Escherichia coli* by carbon dioxide under pressure. *J Food Sci* **61**, 829–831.
- Barbesti, S., Citterio, S., Labra, M., Baroni, M. D., Neri, M. G. & Sgorbati, S. (2000). Two and three-color fluorescence flow cytometric analysis of immunoidentified viable bacteria. *Cytometry* **40**, 214–218.
- Berney, M., Hammes, F., Bosshard, F., Weilenmann, H. U. & Egli, T. (2007). Assessment and interpretation of bacterial viability by using the LIVE/DEAD BacLight Kit in combination with flow cytometry. *Appl Environ Microbiol* **73**, 3283–3290.
- Devlieghere, F., Vermeiren, L. & Debevere, J. (2004). New preservation technologies: possibilities and limitations. *Int Dairy J* **14**, 273–285.

- Erkmen, O. (2000).** Effect of carbon dioxide pressure on *Listeria monocytogenes* in physiological saline and foods. *Food Microbiol* **17**, 589–596.
- Erkmen, O. & Karaman, H. (2001).** Kinetic studies on the high pressure carbon dioxide inactivation of *Salmonella typhimurium*. *J Food Eng* **50**, 25–28.
- Ferrentino, G. & Spilimbergo, S. (2011).** High pressure carbon dioxide pasteurization of solid foods: current knowledge and future outlooks. *Trends Food Sci Technol* **22**, 427–441.
- Foladori, P., Quaranta, A. & Ziglio, G. (2008).** Use of silica microspheres having refractive index similar to bacteria for conversion of flow cytometric forward light scatter into biovolume. *Water Res* **42**, 3757–3766.
- Foladori, P., Bruni, L., Tamburini, S. & Ziglio, G. (2010).** Direct quantification of bacterial biomass in influent, effluent and activated sludge of wastewater treatment plants by using flow cytometry. *Water Res* **44**, 3807–3818.
- Gandhi, M. & Chikindas, M. L. (2007).** *Listeria*: a foodborne pathogen that knows how to survive. *Int J Food Microbiol* **113**, 1–15.
- Garcia-Gonzalez, L., Geeraerd, A. H., Spilimbergo, S., Elst, K., Van Ginneken, L., Debevere, J., Van Impe, J. F. & Devlieghere, F. (2007).** High pressure carbon dioxide inactivation of microorganisms in foods: the past, the present and the future. *Int J Food Microbiol* **117**, 1–28.
- Garcia-Gonzalez, L., Geeraerd, A. H., Mast, J., Briers, Y., Elst, K., Van Ginneken, L., Van Impe, J. F. & Devlieghere, F. (2010).** Membrane permeabilization and cellular death of *Escherichia coli*, *Listeria monocytogenes* and *Saccharomyces cerevisiae* as induced by high pressure carbon dioxide treatment. *Food Microbiol* **27**, 541–549.
- Jung, W. Y., Choi, Y. M. & Rhee, M. S. (2009).** Potential use of supercritical carbon dioxide to decontaminate *Escherichia coli* O157:H7, *Listeria monocytogenes*, and *Salmonella typhimurium* in alfalfa sprouted seeds. *Int J Food Microbiol* **136**, 66–70.
- Keer, J. T. & Birch, L. (2003).** Molecular methods for the assessment of bacterial viability. *J Microbiol Methods* **53**, 175–183.
- Kim, H. T., Choi, H. J. & Kim, K. H. (2009).** Flow cytometric analysis of *Salmonella enterica* serotype Typhimurium inactivated with supercritical carbon dioxide. *J Microbiol Methods* **78**, 155–160.
- Klein, D. (2002).** Quantification using real-time PCR technology: applications and limitations. *Trends Mol Med* **8**, 257–260.
- Liao, H., Zhang, F., Liao, X., Hu, X., Chen, Y. & Deng, L. (2010).** Analysis of *Escherichia coli* cell damage induced by HPCD using microscopies and fluorescent staining. *Int J Food Microbiol* **144**, 169–176.
- Mantoan, D. & Spilimbergo, S. (2011).** Mathematical modeling of yeast inactivation of freshly squeezed apple juice under high-pressure carbon dioxide. *Crit Rev Food Sci Nutr* **51**, 91–97.
- Müller, S. & Nebe-von-Caron, G. (2010).** Functional single-cell analyses: flow cytometry and cell sorting of microbial populations and communities. *FEMS Microbiol Rev* **34**, 554–587.
- Nocker, A. & Camper, A. K. (2006).** Selective removal of DNA from dead cells of mixed bacterial communities by use of ethidium monoazide. *Appl Environ Microbiol* **72**, 1997–2004.
- Nocker, A., Sossa-Fernandez, P., Burr, M. D. & Camper, A. K. (2007a).** Use of propidium monoazide for live/dead distinction in microbial ecology. *Appl Environ Microbiol* **73**, 5111–5117.
- Nocker, A., Sossa, K. E. & Camper, A. K. (2007b).** Molecular monitoring of disinfection efficacy using propidium monoazide in combination with quantitative PCR. *J Microbiol Methods* **70**, 252–260.
- Oliver, J. D. (2010).** Recent findings on the viable but nonculturable state in pathogenic bacteria. *FEMS Microbiol Rev* **34**, 415–425.
- Spilimbergo, S. & Bertucco, A. (2003).** Non-thermal bacterial inactivation with dense CO₂. *Biotechnol Bioeng* **84**, 627–638.
- Suo, B., He, Y., Tu, S. I. & Shi, X. (2010).** A multiplex real-time polymerase chain reaction for simultaneous detection of *Salmonella* spp., *Escherichia coli* O157, and *Listeria monocytogenes* in meat products. *Foodborne Pathog Dis* **7**, 619–628.
- Velusamy, V., Arshak, K., Korostynska, O., Oliwa, K. & Adley, C. (2010).** An overview of foodborne pathogen detection: in the perspective of biosensors. *Biotechnol Adv* **28**, 232–254.
- WHO (2007).** *Global Public Health Security in the 21st Century*. Geneva: World Health Organization.
- Wouters, P. C., Bos, A. P. & Ueckert, J. (2001).** Membrane permeabilization in relation to inactivation kinetics of *Lactobacillus* species due to pulsed electric fields. *Appl Environ Microbiol* **67**, 3092–3101.
- Ziglio, G., Andreottola, G., Barbesti, S., Boschetti, G., Bruni, L., Foladori, P. & Villa, R. (2002).** Assessment of activated sludge viability with flow cytometry. *Water Res* **36**, 460–468.

Edited by: D. Mills